



Contents lists available at ScienceDirect

Bioorganic & Medicinal Chemistry

journal homepage: www.elsevier.com/locate/bmc

Natural product-inspired profluorophores for imaging NQO1 activity in tumour tissues

Zhiming Cheng^a, Wagner O. Valença^b, Gleiston G. Dias^b, Jamie Scott^a, Nicole D. Barth^a, Fabio de Moliner^a, Gabriela B.P. Souza^b, Richard J. Mellanby^c, Marc Vendrell^{a,*}, Eufrânio N. da Silva Júnior^{b,*}

^a Centre for Inflammation Research, The University of Edinburgh, EH16 4TJ Edinburgh, UK

^b Institute of Exact Sciences, Department of Chemistry, Federal University of Minas Gerais, Belo Horizonte 31270-901, MG, Brazil

^c Royal (Dick) School of Veterinary Studies, The Roslin Institute, Division of Veterinary Clinical Studies, The University of Edinburgh, Hospital for Small Animals, Easter Bush Veterinary Centre, EH25 9RG Roslin, UK

ABSTRACT

Herein we designed a collection of trimethyl-lock quinone profluorophores as activity-based probes for imaging NAD(P)H:quinone oxidoreductase (NQO1) in cancer cells and tumour tissues. Profluorophores were prepared *via* synthetic routes from naturally-occurring quinones and characterised *in vitro* using recombinant enzymes, to be further validated in cells and fresh frozen canine tumour tissues as potential new tools for cancer detection and imaging.

1. Introduction

Functional fluorophores¹ are powerful tools for early detection of diseases and to enhance the accuracy of medical procedures,² such as fluorescence-guided surgery,³ where new imaging approaches have emerged to improve the definition of tumour margins and increase the effectiveness of surgical tissue resection.^{4,5} Fluorescent probes can be also applied *ex vivo* at the tissue level, providing activity-based readouts of enzymes (e.g. proteases) as diagnostic biomarkers or to monitor disease progression over time. Such approaches are complementary to immunohistochemistry and *in situ* hybridisation, commonly used in pathology labs, in that they provide direct measurements of protein activity rather than only protein expression. In this context, the group of Bogoy recently validated the topical application of fluorescently quenched probes for imaging of cathepsin activity in human biopsy samples from cancer patients.⁶ Whereas these are extremely valuable tools, there are few chemical fluorophores for monitoring non-protease enzymatic activity of tumour cells in intact tissues.

NAD(P)H:quinone oxidoreductase 1 (NQO1), also known as DT-diaphorase, is a flavoprotein recognized for its ability to carry out a two-electron reduction of various quinones to hydroquinones in the presence of the cofactors NADH or NADPH.⁷ Numerous studies have revealed that solid tumours such as cholangiocarcinoma, breast, cervical and lung cancers exhibit drastically higher NQO1 levels than normal tissues.⁸ Therefore, in the recent years, NQO1 has drawn significant attention as a potential biomarker for cancer therapy and

imaging. One of the main strategies for the development of chemical probes targeting NQO1 is the use of trimethyl-lock (TML) quinones to control the release of fluorescent compounds.⁹ Profluorophores are constructed where they undergo the two-electron reduction of the quinone moiety by NQO1 to release a bright fluorescent reporter via an intramolecular lactonization process (Scheme 1A).

TML-quinone optical probes have been developed including derivatives with rhodamine structures and chemiluminescent probes.¹⁰ Reported examples, however, do not consider their application in intact tissue biopsies, where profluorophores must show: 1) fast cell uptake, 2) high selectivity over related enzymes and abundant intracellular biomolecules, 3) rapid activation upon enzymatic reaction, and 4) lack of cross-reactivity against abundant biomolecules. Given the structural complexity of most conventional fluorescent scaffolds, we have addressed the preparation of new profluorophores considering both structural simplification as well as simple synthetic routes. Based on our experience with natural products in medicinal chemistry programmes,¹¹ herein we designed a new family of TML-quinone-based nitrogenated heterocycles derived from lapachol as activity-based profluorophores for NQO1. The chemical design is based on the preparation of fluorescent heterocycles via redox center modification of quinoidal systems to render caged compounds which were further conjugated to the TML-quinone reactive cores (Scheme 1B). Notably, these compounds can be synthesized in only a few steps from available natural products with good recovery yields using simple synthetic routes.

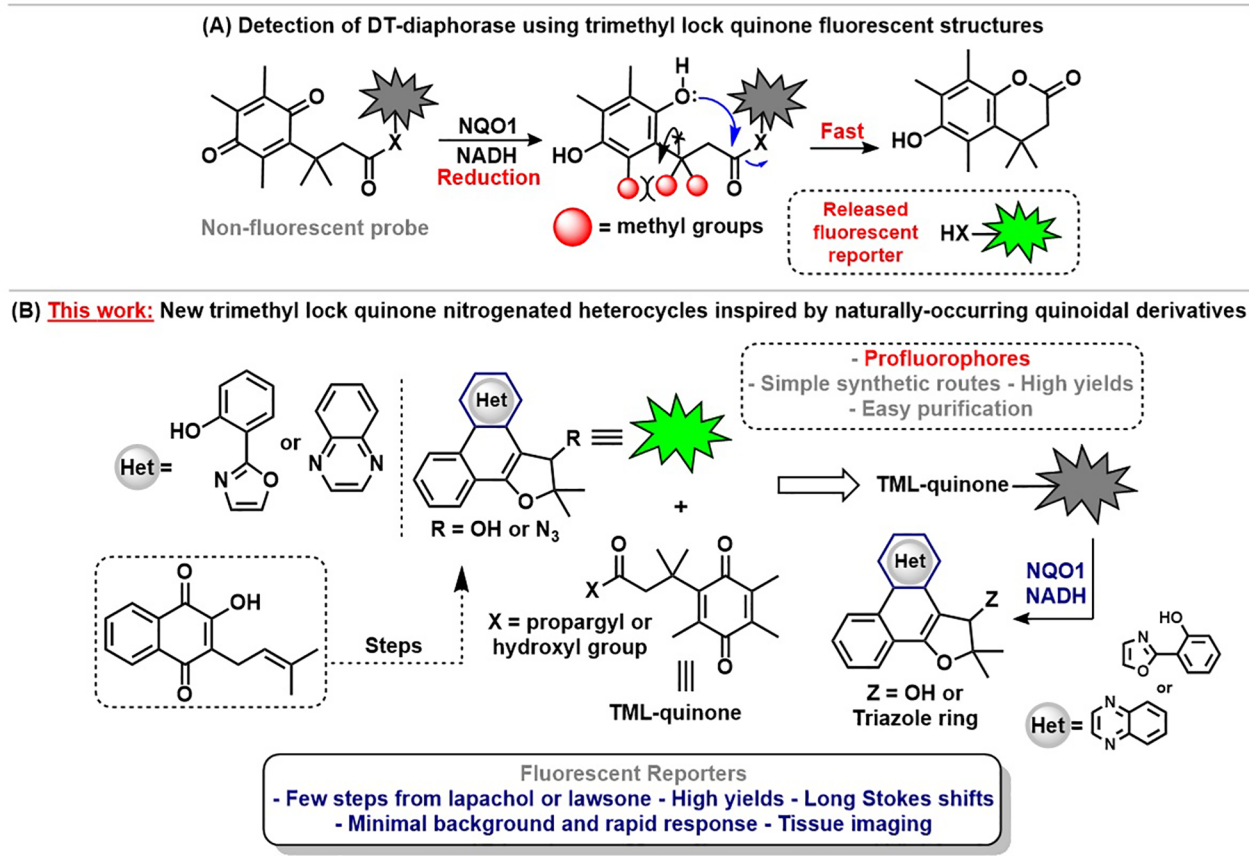
* Corresponding authors.

E-mail addresses: marc.vendrell@ed.ac.uk (M. Vendrell), eufranio@ufmg.br (E.N. da Silva Júnior).

<https://doi.org/10.1016/j.bmc.2019.07.017>

Received 20 May 2019; Received in revised form 8 July 2019; Accepted 10 July 2019

0968-0896/ © 2019 Published by Elsevier Ltd.



Scheme 1. (A) General mechanism involving the trimethyl lock system in enzymatic processes. (B) Synthetic planning used for the preparation of new TML-quinone systems.

2. Results and discussion

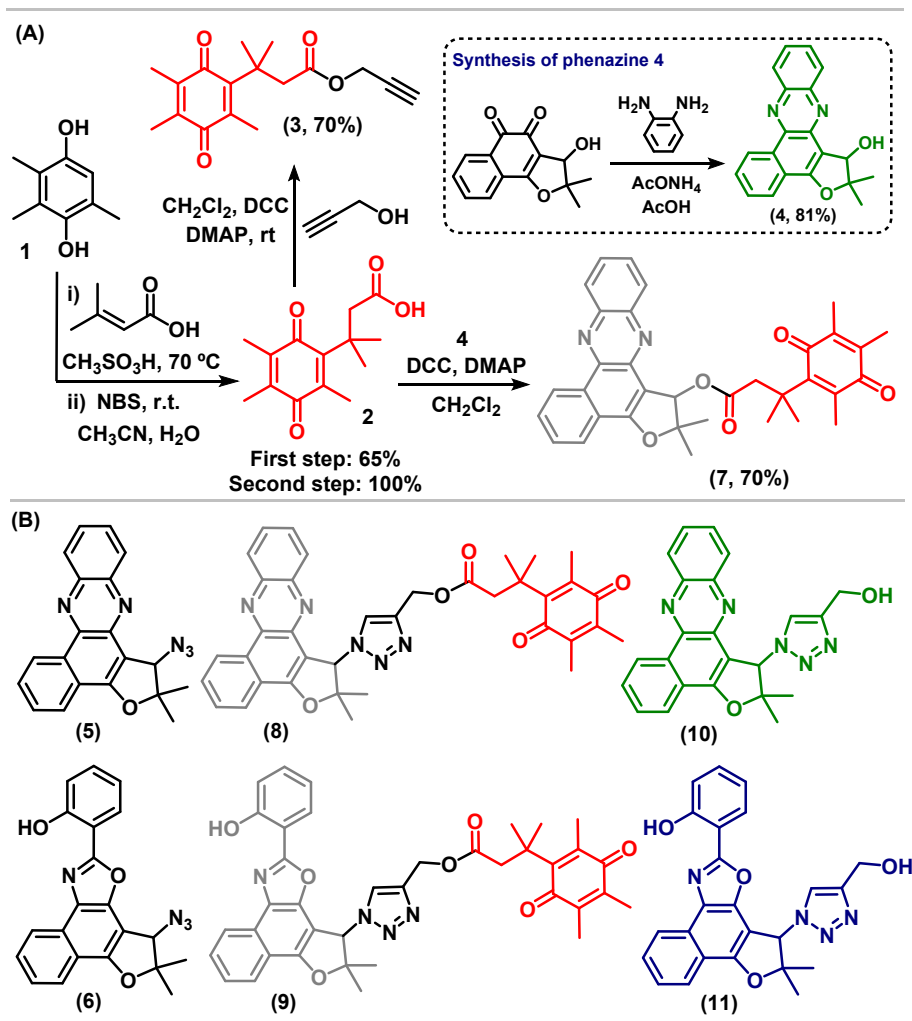
The synthesis of TML-quinone profluorophores was accomplished by a convergent route, using esterification reactions or copper-catalyzed azide-alkyne cycloaddition¹² to couple fluorescent heterocycles and TMLs. Initially, following the method described by Rohde and co-workers,¹³ the TML-quinone **2** was prepared in two steps from the commercially available trimethylhydroquinone **1**. With compound **2** in hands, the alkyne derivative **3** was readily obtained by condensation in the presence of DCC and DMAP (Schemes 2A and S1).¹⁴ As for the heterocycles, phenazine (**4** and **5**) and oxazole (**6**) structures were synthesized from lapachol in good yields by reported methods (Schemes S2–S5).^{15,16} Alternatively, Camara and co-workers have recently described a methodology to prepare nor-lapachol from lawsone,¹⁷ which would allow access to similar phenazine structures. Finally, we generated a small collection of TML-quinone profluorophores (**7–9**) by coupling the TML-quinone moieties **2** and **3** to the corresponding heterocycles (Schemes S6–S8). Furthermore, we also generated the non-reactive fluorescent heterocycles (**4**, **10** and **11**) bearing a free hydroxyl group instead of the TML-quinone core for direct comparative studies (Schemes 2A, S9 and S10).

First, we examined the spectral properties of the TML-quinone profluorophores **7–9**, and compared them to their uncaged counterparts (**4**, **10** and **11**, respectively) (Table S1). All 3 profluorophores showed significant quenching when compared to the quinone-free structures, with fluorescence increases up to 200-fold (Figs. 1 and S1). This behaviour is likely due to the photoinduced electron transfer (PeT) between the fluorescent cores (e.g. phenazine, oxazole) and the TML-quinone moiety, as it has been reported for other TML-quinone fluorescent probes.¹⁸ Next, we then tested their reactivity against

recombinant human NQO1 (hNQO1). Compounds **7–9** were incubated with hNQO1 (1 μM) in Tris-HCl buffer containing NADH (0.1 mM) at 37 $^{\circ}\text{C}$, and we measured their fluorescence emission after 30 min. Notably, compounds **7** and **8** exhibited the highest fluorescence amplification, highlighting that the phenazine core is better tolerated than the oxazole in the hNQO1 binding pocket. The profluorophores also showed a differential behaviour dependent on the linkage between the TML-quinone moiety and the phenazine structure, being the short spacer in profluorophore **7** better tolerated than its triazole-based counterpart in profluorophore **8**. Compound **7** showed a fast response to active hNQO1 (i.e. in the presence of its cofactor NADH), reaching 50% of its maximal response only after 10 min (Figs. 1 and S2). These results are in agreement with the literature in which the enzyme hNQO1 is only active in the presence of its cofactor NADH.¹⁹

In order to confirm that the fluorescence emission of **7** was due to its reaction with hNQO1 and the concomitant release of compound **4**, we analysed the enzymatic reaction mixture by HPLC-MS and confirmed the transformation of the non-fluorescent compound **7** to the fluorescent phenazine (**Fig. S3**). Spectroscopic analysis of the pair **4–7** showed absorption and emission maxima wavelengths in the blue and green region of the visible spectrum respectively (λ_{abs} : 425 nm; λ_{em} : 490 nm) with a substantial Stokes shift (> 60 nm) favourable for live-cell imaging.

Then, we assessed the kinetic parameters defining the enzymatic reaction between the profluorophore **7** and hNQO1. We plotted the initial rate of formation of the phenazine **4** against different concentrations of **7** in Tris-HCl buffer at 37 $^{\circ}\text{C}$ (**Fig. 2**), and subsequently determined its maximum rate (V_{max}), Michaelis constant (K_{m}) and catalyst rate constant (K_{cat}) (**Fig. 2**). Overall, compound **7** displays a catalytic efficiency in the range of 170,000 $\text{M}^{-1} \text{min}^{-1}$, which is in the



Scheme 2. (A) Example of synthetic route used for the preparation of TML-quinone-based heterocycles. (B) Clickable heterocycles 5 and 6 and caged vs uncaged pairs 8 vs 10 and 9 vs 11.

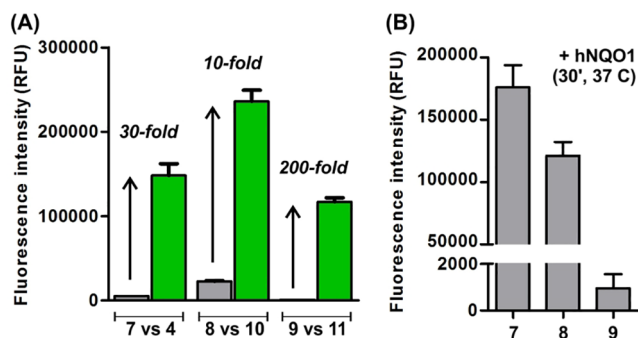


Fig. 1. (A) Fluorescence fold increase between the pairs of compounds 4–7, 10–8 and 11–9. (B) Fluorescence intensity of compounds 7, 8 and 9 upon enzymatic activation by hNQO1 (1 μ M) and NADH (0.1 mM) for 30 min 37 $^{\circ}$ C ($\lambda_{exc.}$: 405 nm, $\lambda_{em.}$: 490 nm). Data presented as mean values and error bars as s.e.m (n = 3).

range or better than most TML-quinone fluorescent probes reported to date.^{10,20} Further experiments were conducted to assess the selectivity of the TML-quinone 7 for hNQO1 over related enzymes and intracellular redox biomolecules. In addition to incubating 7 with hNQO1 in the presence of NADH, we also assessed its fluorescence response in the presence of dicoumarol, a known inhibitor of hNQO1.²¹ A significant decrease in the fluorescence amplification was observed by

inhibition of hNQO1, confirming the reactivity of compound 7 against this enzyme. We also tested its response against hNQO2, another quinone reductase that can be found in the cytosol of mammalian cells and is able to reduce quinone structures.²² Notably, compound 7 showed no cross-reactivity with hNQO2, confirming its specificity for hNQO1 (Fig. 2). Moreover, we also examined whether other biologically-relevant reducing agents could lead to the activation of the pro-fluorophore 7. We incubated compound 7 with a large excess of multiple redox biomolecules (e.g. NADH, ascorbic acid, γ -cysteine and glutathione) and monitored the resulting fluorescence emission. Under these conditions, we did not detect any significant fluorescence amplification, proving the suitability of compound 7 to specifically monitor the activity of hNQO1 in live cells by fluorescence readouts.

Encouraged by these results, we employed compound 7 for fluorescence imaging of hNQO1 activity in live human cells expressing different levels of the enzyme. Specifically, we used HeLa (human cervical cancer) and HL-60 (human leukemia) cell lines due to their reported high expression and low expression of hNQO1, respectively.^{23,24} We acquired fluorescence microscopy images of both cell lines under the same experimental conditions (30 min incubation, 37 $^{\circ}$ C), and observed much brighter signals in the cytosol of hNQO1-positive cells (i.e. HeLa), in line with literature reports describing the cytoplasm as the main subcellular region for hNQO1 enzymes (Fig. 3).²⁴ Plot profile analysis with the red-fluorescent counterstain DRAQ5 was used to clarify the differential fluorescence intensity of the TML-quinone 7 in both cell

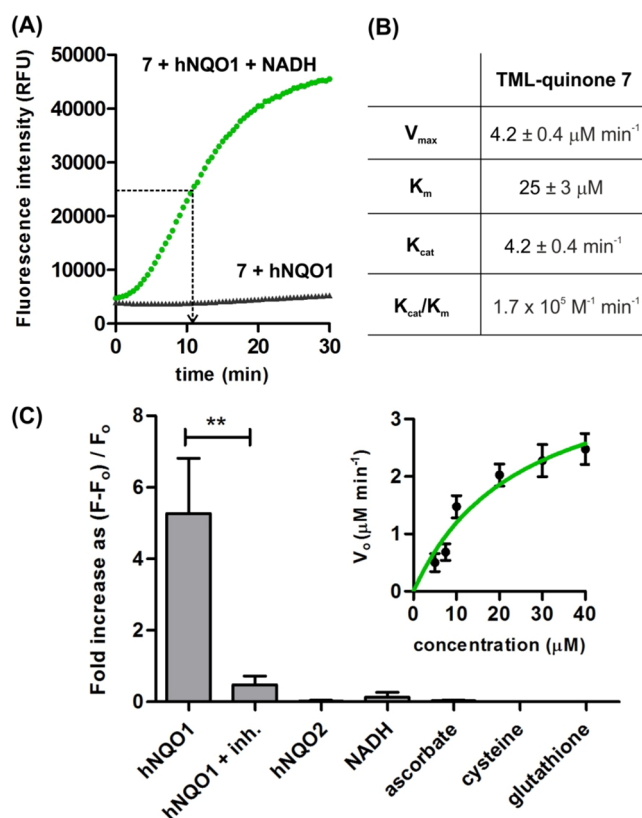


Fig. 2. (A) Time dependence enzymatic activation assay of compound 7 (50 μM) with hNQO1 (1 μM) and NADH (0.1 mM) in Tris-HCl buffer for 30 min at 37 $^{\circ}\text{C}$ (λ_{ex} : 405 nm, λ_{em} : 490 nm). (B) Kinetic parameters of compound 7 upon enzymatic activation by hNQO1. (C) Fluorescence fold increase of compound 7 (50 μM) after incubation with different enzymes and biomolecules. hNQO1 (1 μM) was added with NADH (0.1 mM) and with or without inhibitor [dicoumarol, 100 μM]. hNQO2 was added with its cofactor 1-methylnicotinamide (0.1 mM). Other biomolecules were tested at 1 mM in Tris-HCl buffer (λ_{ex} : 405 nm, λ_{em} : 490 nm). Inset Kinetic plot of the initial rate, V_0 , against different concentrations of compound 7 [5 μM , 7.5 μM , 10 μM , 20 μM , 30 μM and 40 μM]. Data presented as mean values and error bars as s.e.m (n = 3). ** for p < 0.01.

types. Finally, in order to confirm that the intracellular activation of the profluorophore 7 was due to its reaction with hNQO1, we pre-incubated HeLa cells with dicoumarol (25 μM , 1 h) prior to the addition of compound 7. As shown in Fig. 3, the blockage of the activity of hNQO1 in HeLa cells led to a significant reduction of the fluorescence signal, highlighting the reduction of the TML-quinone by active hNQO1 as the main intracellular mechanism for the activation of the profluorophore 7 inside cells.

Finally, we used compound 7 for *in situ* imaging of NQO1 activity in tumour tissues. Fresh frozen canine samples from healthy and adenocarcinoma colorectal tissues were thawed and treated with DRAQ5, a generic red fluorescent cell marker, and compound 7. Notably, tumour tissues presented brighter green fluorescence than healthy tissues. Furthermore, we could confirm that the signal was due to increased NQO1 activity by blocking the response of compound 7 with the NQO1 inhibitor dicoumarol (Fig. 4).

3. Experimental

3.1. Materials and apparatus

Unless otherwise indicated, all common reagents and solvents were used as obtained from commercial suppliers without further purification. All commercial chemicals were purchased from Sigma Aldrich.

Flash column chromatography (FCC) was performed using silica gel (Aldrich 40–63 μm , 230–400 mesh). Thin layer chromatography (TLC) was performed using aluminium backed 60 F254 silica plates. Visualization was achieved by UV fluorescence. Proton nuclear magnetic resonance spectra (^1H NMR) were recorded using Bruker DRX 400 or Bruker Avance III 400 MHz, with 5 mm sample tubes, 298 K, digital resolution of 0.01 ppm. Carbon nuclear magnetic resonance spectra (^{13}C NMR) were recorded at 100 MHz as stated, with 5 mm sample tubes, 298 K, digital resolution of 0.1 ppm. Chemical shifts (δ) are given in parts per million (ppm). Peaks are described as singlets (s), doublets (d), double doublets (dd), triplets (t), double triplets (dt), and multiplets (m). ^1H and ^{13}C NMR spectra were referenced to the appropriate residual solvent peak or TMS peak. Coupling constants (J) were quoted to the nearest 0.5 Hz. Mass spectra were recorded using a Bruker Daltonics FT-ICRMS Apex 4e 7.0 T FT-MS (ESI⁺ mode) and Shimadzu GCMS QP2010+ (EI⁺ mode). Infrared spectra were recorded on a Perkin Elmer Spectrum One FTIR spectrometer as thin films or solids compressed on a diamond plate. Melting points were determined using Stuart SMP30 melting point apparatus and are uncorrected.

4. Synthetic experiments

4.1. Synthesis of 6-hydroxy-4,4,5,7,8-peptamethyl-chroman-2-one

Compound 1' was prepared according to the methodology described by Rohde and co-workers with minor modifications¹³ from the reaction of the 2,3,5-trimethylhydroquinone with 3,3-dimethylacrylic acid and methanesulfonic acid. A mixture of the 2,3,5-trimethylhydroquinone (2 g, 13.1 mmol) with 3,3-dimethylacrylic acid (1.45 g, 14.5 mmol) and methanesulfonic acid (10 mL) was stirred at 85 $^{\circ}\text{C}$ for 3 h and then cooled to room temperature. The mixture was extracted with CH_2Cl_2 (2 \times 100 mL) and combined organic layer was washed with saturated NaHCO_3 (3 \times 100 mL) and water (3 \times 100 mL) and dried over MgSO_4 . After filtration and evaporation, a residue was obtained and recrystallized from hexane and CH_2Cl_2 (5:1, v/v) to give the desired product as a white solid (2.0 g, 8.5 mmol, 65% yield); m.p. 180–182 $^{\circ}\text{C}$. ^1H NMR (400 MHz, CDCl_3 , 303 K) δ : 4.72 (s, 1H), 2.55 (s, 2H), 2.37 (s, 3H), 2.23 (s, 3H), 2.19 (s, 3H), 1.46 (s, 6H). ^{13}C NMR (100 MHz, CDCl_3 , 303 K) δ : 169.1, 149.0, 143.8, 128.5, 123.7, 122.1, 119.1, 46.3, 35.7, 27.9, 14.6, 12.5, 12.2. Data are consistent with those reported in the literature.¹³ See SI for synthetic route.

4.2. Synthesis of 3-methyl-3-(2,4,5-trimethyl-3,6-dioxocyclohexa-1,4-dienyl)butanoic

Compound 2 was prepared according to the methodology described by Rohde and co-workers with minor modifications.¹³ Compound (1') (1.58 g, 6.74 mmol) and *N*-bromosuccinimide (1.26 g, 7.08 mmol) were added to a flask containing a mixture of acetonitrile (15 mL) and water (3 mL) and kept under stirring at room temperature. After 30 min, solvents were evaporated under reduced pressure. The residue obtained was recrystallized from CH_2Cl_2 and AcOEt (8:1, v/v) to give the desired product as a yellow solid (2.69 g, 10.8 mmol, 100% yield); m.p. 195–197 $^{\circ}\text{C}$. ^1H NMR (400 MHz, CDCl_3 , 303 K) δ : 9.25 (s, 1H), 2.99 (s, 2H), 2.12 (s, 3H), 1.93 (s, 3H), 1.90 (s, 3H), 1.41 (s, 6H). ^{13}C NMR (100 MHz, CDCl_3 , 303 K) δ : 191.0, 187.7, 178.6, 152.3, 143.2, 139.2, 138.6, 47.5, 38.2, 29.7, 29.0, 14.5, 12.7, 12.3. Data are consistent with those reported in the literature.¹³

4.3. Synthesis of prop-2-yn-1-yl-3-methyl-3-(2,4,5-trimethyl-3,6-dioxocyclohexa-1,4-dien-1-yl) butanoate

Compound 3 was prepared according to the methodology described by Zhang and co-workers.¹⁴ To a solution of compound 2 (0.400 g, 1.60 mmol) and DCC (0.363 g, 1.76 mmol) in CH_2Cl_2 (10 mL) was added DMAP (0.022 g, 0.16 mmol), stirring at room temperature. After

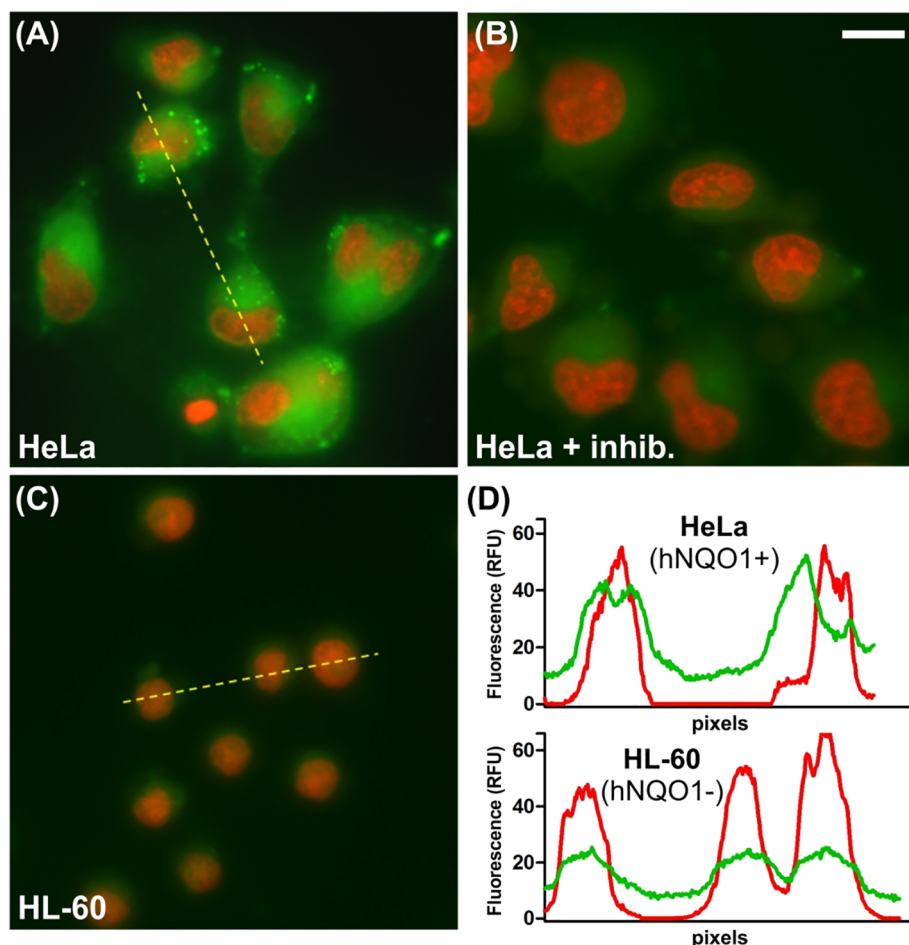


Fig. 3. (A–C) Fluorescence microscopy images of HeLa cells (with and without pre-incubation of dicoumarol, 25 μ M, 1 h) and HL-60 cells after incubation with compound **7** (green, 50 μ M) for 30 min at 37 $^{\circ}$ C. Nuclei staining was achieved by incubating the cells with DRAQ5 (red, 1 μ M). (D) Plot profile analysis of the staining of compound **7** (green) and DRAQ5 (red) in HeLa cells (image (A), top) and HL-60 cells (image (C), bottom) as indicated by the yellow line transections. Scale bar: 20 μ m.

30 min, propargyl alcohol (3 equivalents) was added and the mixture was stirred overnight. After reaction finished, the mixture was poured onto water and extracted with ethyl acetate (3×20 mL). The organic phases were combined, dried over Na_2SO_4 , and concentrated under vacuum. The crude product was purified by column chromatography and the product **3** was obtained as an oil (70% yield). ^1H NMR (400 MHz, CDCl_3 , 303 K) δ : 4.58 (d, $J = 2.4$ Hz, 2H), 3.02 (s, 2H), 2.41 (t, $J = 2.4$ Hz, 1H), 2.15 (s, 3H), 1.97 (s, 6H), 1.45 (s, 6H). ^{13}C NMR (100 MHz, CDCl_3 , 303 K) δ : 191.0, 187.6, 172.0, 152.2, 143.2, 139.3, 138.7, 77.7, 74.9, 51.8, 47.5, 38.6, 29.1, 14.5, 12.8, 12.3. EI/HRMS (m/z) $[\text{M} + \text{H}]^+$: 289.1430. Cald. for $[\text{C}_{17}\text{H}_{21}\text{O}_4]^+$: 289.1434.

4.4. Extraction and purification of the natural product lapachol

Lapachol was initially extracted from the heartwood of *Tabebuia* sp. (*Tecoma*) and purified by a series of recrystallizations. Initially, nor-lapachol was synthesized by Hooker oxidation methodology²⁵ and data are consistent with those reported in the literature.²⁶ Nor-lapachol was obtained as an orange solid (160 mg, 0.7 mmol, 70% yield); m.p. 121–122 $^{\circ}$ C. ^1H NMR (400 MHz, CDCl_3 , 303 K) δ : 8.13 (ddd, $J = 7.5$, 1.5 and 0.5 Hz, 1H), 8.10 (ddd, $J = 7.5$, 1.5 and 0.5 Hz, 1H), 7.76 (td, $J = 7.5$, 7.5 and 1.5 Hz, 1H), 7.69 (td, $J = 7.5$, 7.5 and 1.5 Hz, 1H), 6.03–5.99 (m, 1H), 2.0 (d, $J = 1.5$ Hz, 3H), 1.68 (d, $J = 1.2$ Hz, 3H). ^{13}C NMR (100 MHz, CDCl_3 , 303 K) δ : 184.7, 181.5, 151.1, 143.6, 134.9, 133.0, 132.9, 129.5, 126.9, 126.0, 120.9, 113.6, 26.5, 21.7. Data are consistent with those reported in the literature.²⁶

4.5. Synthesis of 3-azido-2,2-dimethyl-2,3-dihydro-1,2-benzofuran-4,5-dione, 3-azido-nor- β -lapachone

To a solution of nor-lapachol (228 mg, 1.0 mmol) in 25 mL of chloroform, 2 mL of bromine was added. The bromo intermediate precipitated immediately as an orange solid. After removal of bromine, by adding dichloromethane and then removing the organic solvent with dissolved bromine by rotary evaporator, an excess of sodium azide (2 mmol) was added in CH_2Cl_2 and the mixture was stirred overnight. The crude reaction mixture was poured into 50 mL of water. The organic phase was extracted with organic solvent, dried over anhydrous Na_2SO_4 , filtered, and evaporated under reduced pressure. The azido product was obtained after recrystallization as an orange solid (263 mg, 0.98 mmol, 98% yield); m.p. 200–202 $^{\circ}$ C. ^1H NMR (400 MHz, CDCl_3 , 303 K) δ : 8.14 (ddd, $J = 6.9$, 2.1 and 0.9 Hz, 1H), 7.72–7.65 (m, 3H), 4.77 (s, 1H), 1.67 (s, 3H), 1.55 (s, 3H). ^{13}C NMR (100 MHz, CDCl_3 , 303 K) δ : 180.3, 175.2, 170.2, 134.5, 132.7, 131.1, 113.5, 129.5, 125.1, 126.7, 95.5, 67.3, 27.1, 21.9. Data are consistent with those reported in the literature.²⁷ Nor-lapachol can be prepared from lawsone as described by Camara and co-workers.¹⁷ See SI for synthetic route.

4.6. Synthesis of 2,2-dimethyl-1,2-dihydrobenzo[*a*]furo[2,3-*c*]phenazin-1-ol

Compound **4** was prepared following procedure described above. A mixture of the 3-hydroxy-nor- β -lapachone (244 mg, 1.00 mmol),

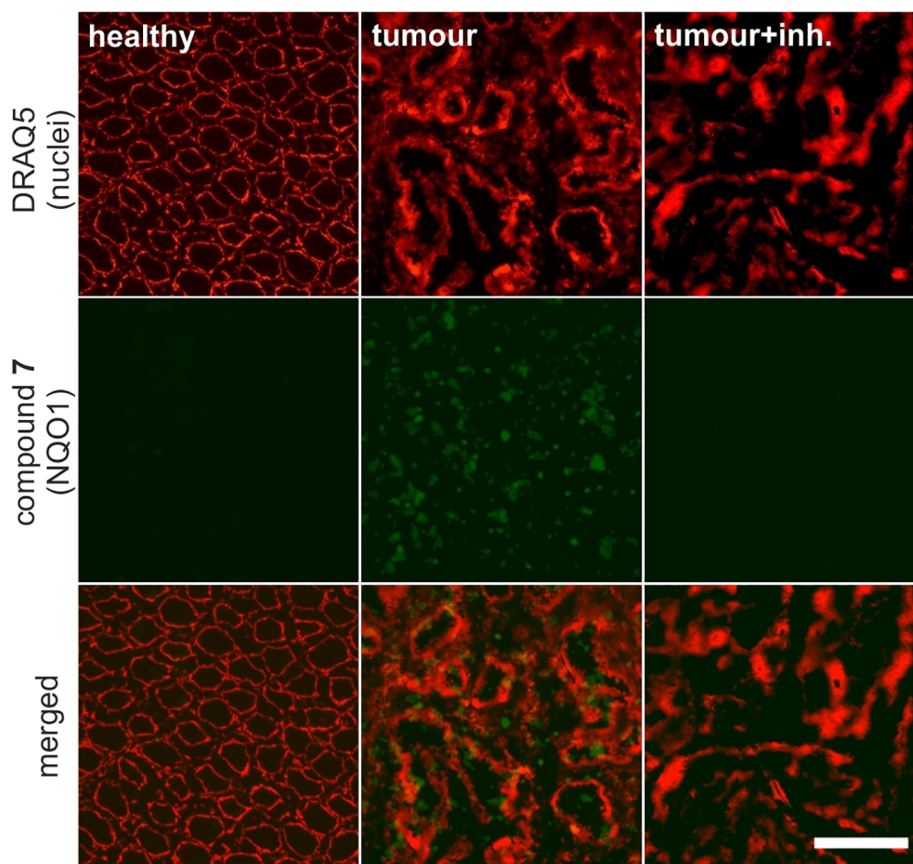


Fig. 4. Fluorescence microscopy images of canine healthy tissue and adenocarcinoma colorectal tissue after incubation with DRAQ5 (red) and compound 7 (500 μ M, green). Specificity of the green fluorescent signal was confirmed by treatment with dicoumarol (100 μ M, 1 h). Scale bar: 275 μ m.

sodium acetate (156 mg, 1.90 mmol), *ortho*-phenylenediamine (119 mg, 1.10 mmol) in 3 mL of glacial acetic acid was stirred and monitored by silica gel thin-layer chromatography (TLC). After, the crude reaction product was poured into water and the precipitate formed was filtrate and then purified in silica gel chromatography, using a mixture of hexane–ethyl acetate, increasing polarity. Compound (4) was obtained as a yellow solid (256 mg, 0.81 mmol, 81% yield); m.p. 156–158 °C. ^1H NMR (400 MHz, CDCl_3 , 303 K) δ : 9.27 (d, J = 8.0 Hz, 1H), 8.21–8.09 (m, 3H), 7.82 (t, J = 8.0 Hz, 2H), 7.67 (s, 2H), 5.70 (s, 1H), 4.12 (s, 1H), 1.81 (s, 3H), 1.61 (s, 3H). ^{13}C NMR (100 MHz, CDCl_3 , 303 K) δ : 140.1, 132.5, 130.6, 130.1, 130.0, 129.5, 128.4, 127.2, 126.1, 124.8, 123.3, 114.0, 93.8, 27.2, 21.3. EI/HRMS (m/z) [$M + H$] $^+$: 317.1279. Cald. for $[\text{C}_{20}\text{H}_{17}\text{N}_2\text{O}_2]^+$: 317.1285.

4.7. Synthesis of 1-azido-2,2-dimethyl-1,2-dihydrobenzo[*a*]furo[2,3-*c*]phenazine

Compound 5 was prepared according to the classical methodology described by Hooker²⁸ from the reaction of the 3-azido-nor- β -lapachone with *ortho*-phenylenediamine. A mixture of the 3-azido-nor- β -lapachone (0.5 mmol), sodium acetate (0.95 mmol), *ortho*-phenylenediamine (0.55 mmol) in 3 mL of glacial acetic acid was stirred and monitored by silica gel thin-layer chromatography (TLC). After, the crude reaction product was poured into water and the precipitate formed was filtrate and then purified in silica gel chromatography, using a mixture of hexane–ethyl acetate, increasing polarity. Compound (5) was obtained as a yellow solid (170.5 mg, 0.5 mmol, 100% yield); m.p. 246–248 °C. ^1H NMR (400 MHz, CDCl_3 , 303 K) δ : 9.38 (d, J = 8.0 Hz, 1H), 8.29 (dd, J = 7.2 and 1.2 Hz, 1H), 8.21 (dd, J = 7.2 and 1.6 Hz, 1H), 8.09 (d, J = 7.6 Hz, 1H), 7.86–7.74 (m, 4H), 5.37 (s, 1H), 1.76 (s, 3H), 1.59 (s, 3H). ^{13}C NMR (100 MHz, CDCl_3 , 303 K) δ : 159.3, 142.8,

142.7, 141.2, 140.5, 132.9, 130.3, 129.9, 129.5, 128.9, 128.6, 126.2, 124.5, 123.2, 92.3, 69.9, 27.6, 22.7. EI/HRMS (m/z) [$M + H$] $^+$ 342.0921. Cald for $[\text{C}_{29}\text{H}_{23}\text{N}_5\text{O}_2]^+$: 342.1310.

4.8. Synthesis of 2-(4-azido-5,5-dimethyl-4,5-dihydrofuro[3',2':3,4]naphtho[1,2-*d*]oxazol-2-yl)phenol, (compound 6)

To a solution of 3-azido-nor- β -lapachone (1.0 mmol) in acetic acid (10 mL), salicylaldehyde (244 mg, 0.2 mL, 2.0 mmol) was added, and the mixture was heated to 70 °C; at this point, ammonium acetate (1.54 g, 20 mmol) was slowly added, and the temperature was maintained at 110 °C. All the reactions were monitored by thin layer chromatography and it was observed that after four hours all the starting material was consumed. At this point, the reaction was cooled to room temperature and extracted with dichloromethane and dried with Na_2SO_4 . The solvent was removed under reduced pressure to afford the crude product, which was purified on a silica column using a gradient mixture of hexane/ethyl acetate as eluent (1% of ethyl acetate in hexane). Compound (6) was obtained as a white solid (196 mg, 0.7 mmol, 72% yield); m.p. 169–170 °C. ^1H NMR (400 MHz, CDCl_3 , 303 K) δ : 11.38 (s, 1H), 8.44 (ddd, J = 8.3, 1.2 and 0.8 Hz, 1H), 8.11 (ddd, J = 8.3, 1.2 and 0.8 Hz, 1H), 7.71 (ddd, J = 8.3, 7.0 and 1.2 Hz, 1H), 7.55 (ddd, J = 8.3, 7.0 and 1.2 Hz, 1H), 8.06 (ddd, J = 7.9, 1.7 and 0.4 Hz, 1H), 7.42 (ddd, J = 8.3, 7.3 and 1.7 Hz, 1H), 7.15 (ddd, J = 8.3, 1.1 and 0.4 Hz, 1H), 7.03 (ddd, J = 7.9, 7.3 and 1.1 Hz, 1H), 5.13 (s, 1H), 1.73 (s, 3H), 1.58 (s, 3H). ^{13}C NMR (100 MHz, CDCl_3 , 303 K) δ : 160.6, 157.7, 155.5, 143.2, 132.7, 130.1, 128.6, 126.6, 126.5, 125.4, 123.4, 122.5, 119.7, 119.1, 117.3, 111.1, 102.7, 91.4, 69.4, 27.4, 22.3. EI/HRMS (m/z) [$M + H$] $^+$: 373.1285. Cald. for $[\text{C}_{21}\text{H}_{17}\text{N}_4\text{O}_3]^+$: 373.1300. Data are consistent with those reported in the literature previously described by our group.¹⁶

4.9. Synthesis of 2,2-dimethyl-1,2-dihydrobenzo[a]furo[2,3-c]phenazin-1-yl 3-methyl-3-(2,4,5-trimethyl-3,6-dioxocyclohexa-1,4-dien-1-yl)butanoate, (compound 7)

N,N' -Dicyclohexylcarbodiimide (31 mg, 0.15 mmol) and trimethyl lock quinone (70 mg, 0.2 mmol) were dissolved in 3 mL of CH_2Cl_2 at 0°C under stirring until precipitation (20 min). Separately, 4-(dimethylamino)pyridine (10 mg, 0.1 mmol) and 2,2-dimethyl-1,2-dihydrobenzo[a]furo[2,3-c]phenazin-1-ol (4), (63 mg, 0.2 mmol) were dissolved in 5 mL of CH_2Cl_2 under stirring for 20 min, then added dropwise for 10 min to DCC solution at 0°C . The mixture was heated to 25°C and kept under stirring for 24 h. The mixture was extracted with CH_2Cl_2 and water and dried over Na_2SO_4 . Solvent was evaporated under reduced pressure and the crude was purified under silica gel 60 and *n*-hexane/EtOAc 25:1 to provide compound (7) as a yellow solid (66.8 mg, 0.12 mmol, 60% yield); m.p. $205\text{--}207^\circ\text{C}$. ^1H NMR (400 MHz, CDCl_3 , 303 K) δ : 9.37 (d, $J = 8.0$ Hz, 1H), 8.30–8.28 (m, 1H), 8.08 (d, $J = 8.0$ Hz, 1H), 8.03–8.01 (m, 1H), 7.86–7.74 (m, 4H), 6.65 (s, 1H), 3.64 (d, $J = 16.0$ Hz, 1H), 2.47 (d, $J = 16.0$ Hz, 1H), 1.58 (s, 3H), 1.54–1.52 (m, 9H), 1.39 (s, 3H), 1.28 (s, 3H), 0.97 (s, 3H). ^{13}C NMR (100 MHz, CDCl_3 , 303 K) δ : 190.6, 185.7, 172.0, 160.1, 151.6, 142.4, 142.1, 142.0, 140.6, 140.3, 138.3, 137.3, 133.1, 130.1, 130.0, 129.8, 129.5, 128.4, 128.3, 126.3, 124.2, 122.7, 110.4, 78.3, 48.3, 38.5, 28.4, 28.3, 25.9, 21.0, 13.7, 12.0, 11.0. EI/HRMS (m/z) [$M + H$] $^+$: 549.2383. Cald. for $[\text{C}_{34}\text{H}_{33}\text{N}_2\text{O}_5]^{+}$: 549.2384.

4.10. Synthesis of (1-(2,2-dimethyl-1,2-dihydrobenzo[a]furo[2,3-c]phenazin-1-yl)-1H-1,2,3-triazol-4-yl)methyl 3-methyl-3-(2,4,5-trimethyl-3,6-dioxocyclohexa-1,4-dien-1-yl)butanoate

Compound 8 was prepared according to the classical methodology described by Sharpless, Fokin and co-workers with minor modification.¹² Alkyne (253 mg, 0.87 mmol), $\text{CuSO}_4 \cdot 5\text{H}_2\text{O}$ (12 mg, 0.05 mmol) and sodium ascorbate (25 mg, 0.13 mmol) were added to a solution of azido-phenazine (5) (200 mg, 0.58 mmol) in 10 mL of CH_2Cl_2 : H_2O (1:1). The mixture was stirred at room temperature for 24 h and was monitored by TLC. The organic phase was extracted with CH_2Cl_2 , dried over sodium sulfate and concentrated under reduced pressure. The obtained residue was purified by column chromatography on silica gel, using a gradient mixture of hexane/ethyl acetate with increasing polarity as an eluent. Compound (8) was obtained as a yellow solid (284 mg, 0.45 mmol, 77% yield); m.p. $286\text{--}287^\circ\text{C}$. ^1H NMR (400 MHz, CDCl_3 , 303 K) δ : 9.45 (d, $J = 8.0$ Hz, 1H), 8.30–8.28 (m, 1H), 8.20 (d, $J = 8.0$ Hz, 1H), 8.03–8.00 (m, 1H), 7.92 (t, $J = 7.0$ Hz, 1H), 7.77–7.75 (m, 2H), 7.12 (s, 1H), 6.66 (s, 1H), 5.00 (d, $J = 13.0$ Hz, 1H), 4.96 (d, $J = 13.0$ Hz, 2H), 2.90 (d, $J = 16.3$ Hz, 1H), 2.76 (d, $J = 16.3$ Hz, 1H), 1.97 (s, 3H), 1.86 (s, 3H), 1.80 (s, 3H), 1.77 (s, 3H), 1.26 (s, 3H), 1.23 (s, 3H), 1.14 (s, 3H). ^{13}C NMR (100 MHz, CDCl_3 , 303 K) δ : 190.9, 187.5, 172.6, 160.5, 152.4, 143.1, 142.9, 142.6, 141.7, 141.1, 140.7, 138.9, 138.5, 133.5, 130.4, 130.2, 130.2, 129.9, 129.1, 129.0, 126.4, 124.2, 123.4, 123.1, 108.7, 92.9, 69.0, 57.6, 47.4, 38.2, 28.7, 27.8, 21.7, 14.3, 12.7, 12.2. HRMS (ES $^+$) calculated for $\text{C}_{37}\text{H}_{35}\text{N}_5\text{O}_5$ [$M + H$] $^+$: 630.2710; found: 630.2711.

4.11. Synthesis of (1-(2-(2-hydroxyphenyl)-5,5-dimethyl-4,5-dihydrofuro[3',2':3,4]naphtho[1,2-d]oxazol-4-yl)-1H-1,2,3-triazol-4-yl)methyl-3-methyl-3-(2,4,5-trimethyl-3,6-dioxocyclohexa-1,4-dien-1-yl)butanoate

Compound 9 was prepared following procedure described above.¹² Compound (9) was obtained as a yellow oil (184 mg, 0.5 mmol, 80% yield). ^1H NMR (400 MHz, CDCl_3 , 303 K) δ : 11.27 (s, 1H), 8.50 (d, $J = 8.3$ Hz, 1H), 8.18 (d, $J = 8.3$ Hz, 1H), 7.86 (d, $J = 8.0$ Hz, 1H), 7.80 (t, $J = 7.2$ Hz, 1H), 7.65 (t, $J = 8.0$ Hz, 1H), 7.12 (d, $J = 8.3$ Hz, 1H), 7.07 (s, 1H), 6.97 (t, $J = 8.0$ Hz, 1H), 6.48 (s, 1H), 5.02 (s, 2H), 2.93 (d, $J = 16.3$ Hz, 1H), 2.82 (d, $J = 16.3$ Hz, 1H), 2.01 (s, 3H), 1.87 (s, 3H), 1.79 (s, 3H), 1.76 (s, 3H), 1.27 (s, 3H), 1.23 (s, 3H), 1.21 (s, 3H). ^{13}C

NMR (100 MHz, CDCl_3 , 303 K) δ : 190.9, 187.6, 172.7, 161.3, 158.0, 156.4, 152.3, 143.4, 143.1, 142.6, 139.0, 138.7, 133.3, 131.0, 129.5, 127.3, 126.9, 126.2, 123.7, 122.9, 120.0, 119.3, 117.6, 111.0, 101.1, 92.0, 68.6, 57.5, 47.5, 38.3, 28.8, 27.5, 21.5, 14.4, 12.7, 12.3. EI/HRMS (m/z) [$M + H$] $^+$: 661.2646. Cald. for $[\text{C}_{38}\text{H}_{36}\text{N}_4\text{O}_4]^{+}$: 661.2657.

4.12. Synthesis of (1-(2,2-dimethyl-1,2-dihydrobenzo[a]furo[2,3-c]phenazin-1-yl)-1H-1,2,3-triazol-4-yl)methanol

Compound 10 was prepared following procedure described above.¹² Compound 10 was obtained as a yellow solid (122 mg, 0.36 mmol, 70% yield); m.p. $291\text{--}292^\circ\text{C}$. ^1H NMR (400 MHz, $\text{DMSO}-d_6$, 303 K) δ : 9.34 (d, $J = 7.5$ Hz, 1H), 8.30 (dd, $J = 3.4$ and 6.5 Hz, 1H), 8.16 (d, $J = 6.5$ Hz, 1H), 8.03–7.95 (m, 3H), 7.89 (s, 1H), 7.86 (dd, $J = 3.4$ and 6.5 Hz, 2H), 6.63 (s, 1H), 5.72 (s, 1H), 4.41 (d, $J = 5.6$ Hz, 2H), 1.73 (s, 3H), 1.14 (s, 3H). ^{13}C NMR (100 MHz, $\text{DMSO}-d_6$, 303 K) δ : 160.4, 148.5, 142.6, 142.4, 141.2, 140.2, 133.0, 131.5, 131.3, 130.7, 130.2, 129.8, 128.9, 125.4, 124.6, 123.6, 123.6, 110.2, 93.5, 68.1, 55.6, 27.6, 21.6. HRMS (ES $^+$) calculated for $\text{C}_{23}\text{H}_{19}\text{N}_5\text{O}_2$ [$M + H$] $^+$: 398.1613; found: 398.1612.

4.13. Synthesis of 2-(4-(4-(hydroxymethyl)-1H-1,2,3-triazol-1-yl)-5,5-dimethyl-4,5-dihydrofuro[3',2':3,4]naphtho[1,2-d]oxazol-2-yl)phenol

Compound 11 was prepared following procedure described above.¹² Compound (11) was obtained as a white solid (69 mg, 0.18 mmol, 40% yield); m.p. $297\text{--}298^\circ\text{C}$. ^1H NMR (400 MHz, $\text{DMSO}-d_6$, 303 K) δ : 10.99 (s, 1H), 8.55 (d, $J = 8.3$ Hz, 1H), 8.13 (d, $J = 8.3$ Hz, 1H), 7.92 (s, 1H), 7.86–7.80 (m, 2H), 7.69 (t, $J = 7.3$ Hz, 1H), 7.45 (t, $J = 7.3$ Hz, 1H), 7.11 (d, $J = 8.3$ Hz, 1H), 7.02 (t, $J = 7.3$ Hz, 1H), 6.67 (s, 1H), 5.11 (t, $J = 5.7$ Hz, 1H), 4.48 (d, $J = 5.7$ Hz, 2H), 1.72 (s, 3H), 1.13 (s, 3H). ^{13}C NMR (100 MHz, $\text{DMSO}-d_6$, 303 K) δ : 160.5, 157.4, 156.1, 148.9, 143.7, 133.8, 130.5, 129.7, 127.6, 126.8, 126.6, 123.7, 123.6, 123.1, 119.2, 120.7, 117.8, 111.5, 103.1, 92.5, 67.5, 55.6, 27.5, 21.6. EI/HRMS (m/z) [$M + H$] $^+$: 429.1563. Cald. for $[\text{C}_{24}\text{H}_{20}\text{N}_4\text{O}_4]^{+}$: 429.1557.

5. Procedures, additional spectroscopy and biological assays. In vitro spectral characterization

Spectroscopic data were recorded on a Synergy HT spectrophotometer (Biotek). Compounds were dissolved in the indicated concentrations and spectra were recorded at r.t. Spectra are represented as means from at least two independent experiments with $n = 3$.

6. Enzyme activation assay

hNQO1 was purchased from Sigma-Aldrich. Solutions of $50\ \mu\text{M}$ of compounds 7, 8 and 9 were prepared in a buffer solution (pH 7.4) containing 25 mM Tris, BSA, Tween-20, $5\ \mu\text{M}$ FAD and 0.1 mM NADH. $1\ \mu\text{M}$ of hNQO1 was prepared using the same buffer solution and was pre-incubated at 37°C . $10\ \mu\text{L}$ of each compound was added to $10\ \mu\text{L}$ of hNQO1 solution and the experiments were performed in a 384-well plate at 37°C . The samples were excited at 405 nm and the fluorescence was collected at 490 nm. Fluorescence measurements were collected every 30 s for 30 min.

7. Enzyme kinetics

Solutions of different concentrations of compound 7 ($5\ \mu\text{M}$, $7.5\ \mu\text{M}$, $10\ \mu\text{M}$, $20\ \mu\text{M}$, $30\ \mu\text{M}$ and $40\ \mu\text{M}$) were prepared in a buffer solution (pH 7.4) containing 25 mM Tris, BSA, Tween-20, $5\ \mu\text{M}$ FAD and 0.1 mM NADH. $1\ \mu\text{M}$ of hNQO1 was prepared using the same buffer solution and pre-incubated at 37°C . Each assay was performed by adding $10\ \mu\text{L}$ of compound 7 to $10\ \mu\text{L}$ of hNQO1 solution in a 384-well plate at 37°C . The assay was excited at 405 nm and the fluorescence was collected at 490 nm. Fluorescence measurements were collected every 30 s for the

first 3 min. A calibration curve was obtained by measuring the fluorescence of different concentrations of the compound **4** in the same buffer solution containing hNQO1. A graph of initial rate against concentrations of compound **7** was plotted to determine the maximum rate V_{\max} and Michaelis constant K_m by the nonlinear regression (curve fit) in GraphPad Prism.

8. Selectivity assays

Solutions of 50 μM of compound **7** were prepared in a buffer containing 25 mM Tris pH 7.4, 6 mg/100 mL BSA, 10 μL /100 mL Tween-20, 5 μM FAD, 0.1 mM NADH. 1 μM of hNQO1 was prepared using the same buffer and was pre-incubated with dicoumarol (100 μM) at 37 $^{\circ}\text{C}$ for 1 h. 10 μL of compound **7** was added to 10 μL of hNQO1 solution and the experiments were performed in a 384-well plate at 37 $^{\circ}\text{C}$. 1 mM solutions of known redox biomolecules (Glutathione, L-Ascorbate, L-Cysteine) were prepared using the same buffer solution and were pre-incubated at 37 $^{\circ}\text{C}$ for 30 min. All selectivity assays were performed with excitation at 405 nm and the fluorescence measurements were collected at 490 nm.

9. Fluorescence microscope live-cell imaging

Human HeLa (ATCC[®] CCL-2[™]) and HL-60 (ATCC[®] CCL-240[™]) cells were grown using Dulbecco's Modified Eagle Medium (DMEM) supplemented with 10% fetal bovine serum (FBS), antibiotics (100 U mL⁻¹ penicillin and 100 mg mL⁻¹ streptomycin) and 2 mM L-glutamine in a humidified atmosphere at 37 $^{\circ}\text{C}$ with 5% CO₂. Cells were regularly passaged in T-75 cell culture flasks. For microscopy experiments, cells were plated on glass chamber slides Lab-Tek[™] II (Nunc) the day before imaging, reaching 75%–90% confluence on the day of the experiment. For imaging experiments, a solution of 50 μM of compound **7** were prepared in PBS containing 5 μM of DRAQ5. Cells were incubated for 30 min at 37 $^{\circ}\text{C}$ with 200 μL of solution containing compound **7** and DRAQ5 as indicated, washed once with 200 μL of PBS and imaged under a EVOS FL2 fluorescence microscope using a 40 \times objective. Microscopy images were analysed and processed with ImageJ.

10. Ex vivo tissue imaging

Tissue experiments were approved by the Veterinary Ethical Review Committee (VERC, reference number 126.18). Canine colorectal adenocarcinoma and healthy colon tissues were snap frozen at -80°C and cut into 6 μm -thick slices. Upon thawing, tissues were air dried for 20–30 min at r.t. and placed in a glass coplin jar for fixation in ice cold acetone (10 min). Afterwards, tissues were air dried at r.t. and a hydrophobic circle was drawn around the tissue section with a PAP pen. Tissues were then rehydrated in PBS (3 \times 5 min) at r.t, treated with 0.1% Triton X-100 in PBS for 5 min at r.t, washed with PBS (3 \times 5 min) at r.t, and incubated with DRAQ5 (5 μM) and dicoumarol (100 μM , 100 μL) for 1 h when applicable. Next, tissues were washed with PBS (3 \times 5 min) at r.t, and incubated with compound **7** (500 μM , 100 μL) and NADH (0.1 mM, 100 μL) for 1 h at 37 $^{\circ}\text{C}$ in the dark. After a final washing with PBS (3 \times 5 min) at r.t, coverslips were mounted in ProLong Gold and tissues were imaged under a EVOS FL2 fluorescence microscope using a 10 \times objective. Microscopy images were analyzed with ImageJ.

11. Conclusions

In summary, we have developed a small collection of new trimethyl-lock profluorophores from naturally-occurring quinones as activity-based probes for NQO1. The phenazine derivative **7** showed rapid and selective fluorescence activation upon reaction with NQO1 but not with other biomolecules or closely-related enzymes. Furthermore, we

validated compound **7** for *in situ* fluorescence imaging of NQO1 activity in cancer cells and fresh frozen canine tumour tissues.

Declaration of Competing Interest

None.

Acknowledgements

J.S. and N.D.B. acknowledge funding from the EPSRC and MRC Centre for Doctoral Training in Optical Medical Imaging OPTIMA (EP/L016559/1) and Scottish Funding Council (H14052). R. J. M. was supported by a Wellcome Trust Intermediate Clinical Fellowship (098493/Z/12/Z). M.V. acknowledges funds from an ERC Consolidator Grant (771443) and the Biotechnology and Biological Sciences Research Council (BB/M025160/1). E.N.S.J. acknowledges funding from CNPq 404466/2016-8 and PQ 305741/2017-9, FAPEMIG (PPM-00638-16, PPM-00635-18 and Rede de Pesquisa e Inovação para Bioengenharia de Nanossistemas-RED-00282-16), and Capes-Humboldt research fellowship programme for experienced researchers (Proc. No 88881.145517/2017-01).

Appendix A. Supplementary data

Supplementary data to this article can be found online at <https://doi.org/10.1016/j.bmc.2019.07.017>.

References

- (a) de Moliner F, Kielland N, Lavilla R, Vendrell M. *Angew Chem Int Ed*. 2017;56:3758–3769
(b) Fernández A, Vendrell M. *Chem Soc Rev*. 2016;45:1182–1196
(c) Kielland N, Vendrell M, Lavilla R, Chang Y-T. *Chem Commun*. 2012;48:7401–7403.
- (a) Park S-J, Yeo HC, Kang N-Y, et al. *Stem Cell Res*. 2014;12:730–741
(b) Mendive-Tapia L, Zhao C, Akram AR, et al. *Nat Commun*. 2016;7:10940–10948
(c) Fernandez A, Vermeren M, Humphries D, et al. *Sci*. 2017;3:995–1005
(d) Knoblauch M, Vendrell M, de Leau E, et al. *Plant Physiol*. 2015;167:1211–1220.
- (a) Landau MJ, Gould DJ, Patel KM. *Ann Transl Med*. 2016;4:392
(b) Gao M, Yu F, Lv C, Choo J, Chen L. *Chem Soc Rev*. 2017;46:2237–2271.
- (a) Husa T, Nguyen QT. *Adv Drug Deliv Rev*. 2014;66:90–100
(b) Nguyen QT, Tsien RY. *Nat Rev Cancer*. 2013;13:653–662.
- Mochida A, Ogata F, Nagaya T, Choyke PL, Kobayashi H. *Bioorg Med Chem*. 2018;26:925–930.
- (a) Segal E, Prestwood TR, van der Linden WA, et al. *Chem Biol*. 2015;22:148–158
(b) Withana N, Garland M, Verdoes M, Ofori LO, Segal E, Bogoy M. *Nat Protocols*. 2016;11:184–191.
- Yang Y, Zhang Y, Wu Q, et al. *J Exp Clin Cancer Res*. 2014;33:14.
- (a) Buranrat B, Chau-in S, Prawn A, Puapairoj A, Zeekpudsa P, Kukongviriyapan Y. *Asian Pacifi J Cancer Prev*. 2012;13:131–136
(b) Cui X, Jin T, Wang X, Jin G, Li Z, Lin L. *Oncol Rep*. 2014;2589–2595
(c) Cui X, Li L, Yan G, et al. *BMC Cancer*. 2015;15:244
(d) Yang Y, Wu Q, Cui X, et al. *J Exp Clin Cancer Res*. 2014;33:145.
- (a) Dias GG, King A, de Moliner F, Vendrell M, da Silva Júnior EN. *Chem Soc Rev*. 2018;47:12–27
(b) Regan CJ, Walton DP, Shafaat OS, Dougherty DA. *J Am Chem Soc*. 2017;139:4729–4736.
- (a) Best QA, Johnson AE, Prasai B, Rouillere A, McCarley RL. *Chem ACS. Biol*. 2016;11:231–240
(c) Best QA, Prasai B, Rouillere A, Johnson AE, McCarley RL. *Chem Commun*. 2017;53:783–786
(d) Son S, Won M, Green O, et al. *Angew Chem Int Ed Engl*. 2019;58:1739–1743.
- (a) Dias GG, King A, de Moliner F, et al. *Chem. Soc. Rev*. 2018;47:12–27
(b) de Moliner F, King A, Dias GG, et al. *Front. Chem*. 2018;6:339
(c) Gontijo TB, de Freitas RP, Emery FS, et al. *Bioorg Med Chem Lett*. 2017;27:4446–4456
(d) Dias GG, Rodrigues BL, Resende JM, et al. *Chem Commun*. 2015;51:9141–9144
(e) Vendrell M, Soriano A, Casadó V, et al. *Chem Med Chem*. 2009;4:1514–1522
(f) Yraola F, Ventura R, Vendrell M, et al. *QSAR Comb Sci*. 2004;23:145–152
(g) Vendrell M, Angulo E, Casadó V, Lluís C, Franco R, Albericio F, Royo M. *J Med Chem*. 2007;50:3062–3069.
- Rostovtsev VV, Green LG, Fokin VV, Sharpless KB. *Angew Chem, Int Ed*. 2002;41:2596–2599.
- Rohde RD, Agnew HD, Yeo W-S, Bailey RC, Heath JR. *J Am Chem Soc*. 2006;128:9518–9525.

14. Zhang X, Li X, Li Z, et al. *Org Lett*. 2018;20:3635–3638.
15. (a) Jardim GAM, Calado HDR, Cury LA, da Silva Júnior EN. *Eur J Org Chem*. 2015;703–709
(b) Jardim GAM, Cruz EHG, Valença WO, et al. *J Braz Chem Soc*. 2015;26:1013–1027.
16. Dias GG, Pinho PVB, Duarte HA, et al. *RSC Adv*. 2016;6:76056–76063.
17. David CC, Lins ACS, Silva TMS, et al. *J Braz Chem Soc*. 2019;30:8–18.
18. (a) Truong VX, Li F, Ercole F, Forsythe JS. *Chem Commun*. 2017;53:12076–12079
(b) Okoh OA, Klahn P. *Chem Bio Chem*. 2018;19:1668–1694.
19. Zhang K, Chen D, Ma K, Wu X, Hao H, Jiang S. *J Med Chem*. 2018;61:6983–7003.
20. (a) Prasai B, Silvers WC, McCarley RL. *Anal Chem*. 2015;87:6411–6418
(b) Hettiarachchi SU, Prasai B, McCarley RL. *J Am Chem Soc*. 2014;136:7575–7578.
21. Asher G, Dym O, Tsvetkov P, Adler J, Shaul Y. *Biochemistry*. 2006;45:6372–6378.
22. Bianchet MA, Erdemli SB, Amzel LM. *Vitam Horm*. 2008;78:63–84.
23. Meyer J, Singh K, Cameron A, et al. *Mar drugs*. 2012;10:900–917.
24. Hosoda S, Nakamura W, Hayashi K. *J Biol Chem*. 1974;249:6416–6423.
25. Fieser LF, Fieser M. *J. Am. Chem. Soc*. 1948;70:3215–3222.
26. (a) da Rocha DR, Mota K, da Silva IMCB, Ferreira VF, Ferreira SB, da Silva Fd.C. *Tetrahedron*. 2014;70:3266–3270
(b) Niehues M, Barros VP, Emery Fd.S, Dias-Baruffi M, Assis Md.D, Lopes NP. *Eur. J. Med. Chem*. 2012;54:804–812
(c) Sacau EP, Estévez-Braun A, Ravelo Á.G, Ferro EA, Tokuda H, Mukainaka T, Nishino H. *Bioorg. Med. Chem*. 2003;11:483–488.
27. da Silva EN, Menna-Barreto RFS, Pinto Md.CFR, Silva RSF, Teixeira DV, de Souza MCBV, De Simone CA, De Castro SL, Ferreira VF, Pinto AV. *Eur. J. Med. Chem*. 2008;43:1774–1780.
28. Hooker SC. *J. Chem. Soc., Trans*. 1893;63:1376–1387.